Grape pomace extract induced beige cells in white adipose tissue from rats and in 3T3-L1 adipocytes

Cecilia Rodriguez Lanzi, Diahann Jeanette Perdicaro, María Silvina Landa, Ariel Fontana, Andrea Antoniolli, Roberto Miguel Miatello, Patricia Isabel Oteiza, Marcela Alejandra Vazquez Prieto

PII: S0955-2863(17)30454-0
DOI: doi:10.1016/j.jnutbio.2018.03.001
Reference: JNB 7939

To appear in:

Received date: 2 June 2017
Revised date: 9 February 2018
Accepted date: 1 March 2018

Please cite this article as: Cecilia Rodriguez Lanzi, Diahann Jeanette Perdicaro, María Silvina Landa, Ariel Fontana, Andrea Antoniolli, Roberto Miguel Miatello, Patricia Isabel Oteiza, Marcela Alejandra Vazquez Prieto , Grape pomace extract induced beige cells in white adipose tissue from rats and in 3T3-L1 adipocytes. The address for the corresponding author was captured as affiliation for all authors. Please check if appropriate. Jnb(2017), doi:10.1016/j.jnutbio.2018.03.001

Grape pomace extract induced beige cells in white adipose tissue from rats and in 3T3-L1 adipocytes

Cecilia Rodriguez Lanzi[a1], Diahann Jeanette Perdicaro[a1], María Silvina Landa[b], Ariel Fontana[c], Andrea Antoniolli[c], Roberto Miguel Miatello[a], Patricia Isabel Oteiza[d], Marcela Alejandra Vazquez Prieto[a*]

[a]Laboratorio de Fisiopatología Cardiovascular, Instituto de Medicina y Biología Experimental de Cuyo, National Scientific and Technical Research Council (CONICET) - Facultad de Ciencias Médicas, Universidad Nacional de Cuyo, Mendoza, Argentina.

[b]Department of Molecular Genetics and Biology of Complex Diseases, Institute of Medical Research "Alfredo Lanari," Buenos Aires University and CONICET, Buenos Aires, Argentina

[c]Laboratorio de Bioquímica Vegetal, Instituto de Biología Agrícola de Mendoza, CONICET-Universidad Nacional de Cuyo, M5528AHB Mendoza, Argentina.

[d]Department of Nutrition and Department of Environmental Toxicology, University of California, Davis, CA, USA.

Running title: Grape pomace extract induce browning of white adipose tissue

*Corresponding author:

Marcela Vazquez Prieto, PhD

School of Medicine, National University of Cuyo and IMBECU-CONICET

Av. Libertador 80 M5502JMA Mendoza, Argentina

Phone: ++54 261 4135000 ext. 2686 / Fax: ++54 261 4494047

E-mail: mvazquez@fcm.uncu.edu.ar

[1] These authors contributed equally to this work

Keywords: Grape pomace extract, polyphenols, brown like-adipocytes, mitochondrial biogenesis, high-fat diet

Abbreviations: **AMPK,** AMP kinases; **ATGL,** adipose triglyceride lipase; **BAT,** brown adipose tissue; **Ctrl,** control; **EC,** (-)-epicatechin; **ERK,** extracellular signal-regulated kinase; **eWAT,** epididymal white adipose tissue; **FFA,** Free fatty acids; **GPE,** grape pomace extract; **HFD,** high-fat diet; **MAPK,** mitogen-activated protein kinase; **MCP-1,** monocyte chemotactic protein-1; **NOX,** NADPH oxidasa; **PBS,** phosphate-buffered saline; **PGC-1α,** peroxisome proliferator-activated receptor-γ coactivator-1 α; **PKA,** cAMP-dependent protein kinase ; **PPARγ,** peroxisome proliferator-activated receptor-γ; **PRDM16,** PR domain containing 16; **Q,** quercetin; **SHR,** spontaneously hypertensive rats; **SPB,** systolic blood pressure; **TG,** triglycerides; **TNFα,** tumor necrosis factor α; **TPC,** total phenolic content; **UCP-1,** uncoupling protein 1; **VAT,** visceral adipose tissue; **VEGF-A,** vascular endothelial grow factor A; **VEGF-R2,** vascular endothelial grow factor receptor 2; **WAT,** white adipose tissue

ABSTRACT

This study investigated the effects of a grape pomace extract (GPE) rich in phenolic compounds, on brown-like adipocyte induction and adiposity in spontaneously hypertensive (SHR) and control normotensive Wistar–Kyoto (WKY) rats fed a high fat diet (HFD). HFD consumption for 10 weeks significantly increased epididymal white adipose tissue (eWAT) in WKY but not in SHR rats. Supplementation with GPE (300 mg/kg body weight/day) reduced adipocyte diameter and increased levels of proteins that participate in adipogenesis and angiogenesis, i.e. peroxisome-proliferator activated receptor gamma (PPARγ), vascular endothelial grow factor-A (VEGF-A) and its receptor 2 (VEGF-R2), and partially increased the uncoupling protein 1 (UCP-1) in WKY. In both strains, GPE attenuated adipose inflammation. In eWAT from SHR, GPE increased the expression of proteins involved in adipose tissue "browning" i.e. PPARγ-coactivator-1α (PGC-1α), PPARγ, PR domain containing 16 (PRDM16) and UCP-1. In primary cultures of SHR adipocytes, GPE-induced UCP-1 upregulation was dependent on p38 and ERK activation. Accordingly, in 3T3-L1 adipocytes treated with palmitate the addition of GPE (30 μM) activated the β-adrenergic signaling cascade (PKA, AMPK, p38, ERK). This led to the associated upregulation of proteins involved in mitochondrial biogenesis (PGC-1α, PPARγ, PRDM16 and UCP-1) and fatty acid oxidation (ATGL). These effects were similar to those exerted by (-)-epicatechin and quercetin, major phenolic compounds in GPE. Overall, in HFD-fed rats, supplementation with GPE promoted brown-like cell formation in eWAT and diminished adipose dysfunction. Thus, winemaking residues, rich in bioactive compounds, could be useful to mitigate the adverse effects of HFD-induced adipose dysfunction.

1. Introduction

Increased visceral adiposity plays a crucial role in the physiopathology of insulin resistance, type 2 diabetes, hypertension and cardiovascular disease [1]. White adipose tissue (WAT) is an endocrine organ that stores energy excess as triglycerides. When subcutaneous WAT cannot store more lipid excess, ectopic fat accumulation occurs leading to visceral WAT expansion [2]. Hypertrophy of visceral adipocytes causes the upregulation of adipocytokine expression and secretion (e.g. tumor necrosis factor alpha (TNFα), interleukin 6 (IL-6), resistin, monocyte chemotactic protein-1 (MCP-1)) and promotes oxidative stress (e.g. upregulating the NADPH oxidase (NOX) family of enzymes). All these events contribute to a pro-inflammatory scenario and to the development of local and peripheral insulin resistance [3, 4].

Inflammation impairs WAT angiogenesis and adipogenesis, key events in the expansion of the adipose tissue. The vascular endothelial grow factor-A (VEGF-A) accounts for most of the proangiogenic activity in adipose tissue through its receptor 2 (VEGF-R2). VEGF-R2 activation by VEGF-A may protect from diet-induced insulin resistance by decreasing adipose tissue inflammation through its effect on M2 anti-inflammatory macrophage recruitment. VEGF-A overexpression can also increase brown adipose tissue (BAT) thermogenesis and promote a “BAT-like” phenotype in WAT depots, increasing energy expenditure and therefore reducing obesity [5-7]. Furthermore, peroxisome proliferator-activated receptor-γ (PPARγ) is a central modulator of adipogenesis, enhancing insulin sensitivity and decreasing macrophage adipose infiltration [8, 9].

In contrast to WAT, BAT has the ability to dissipate energy in the form of heat. This capacity is due to the presence of the uncoupling protein 1 (UCP-1), a key determinant of mitochondrial thermogenesis. Interestingly, “brown-like” or “beige” cells can be observed in WAT [10, 11], and are characterized by the presence of multilocular lipid droplets and high number of mitochondria which are associated with a reduction of total adiposity [12, 13]. The emergence of brown-like cells in WAT depots can be triggered by different stimuli such as cold, exercise, pharmacological treatment for example β-adrenergic stimulation or PPARγ agonists [14-17]. All these stimuli have the common capacity to activate the β-adrenergic receptors. Downstream these receptors several proteins are activated, including protein kinase A (PKA), extracellular signal-regulated kinase 1/2 (ERK) and p38 which directly or indirectly activate PPARγ-coactivator-1α (PGC-1α), PPARγ and PR domain containing 16 (PRDM16) that promotes the transcription of genes involved in “browning” i.e UCP-1 [18-20].

Phenolic compounds are widely distributed in fruits and vegetables with several proposed beneficial effects on human health [21-24]. We previously observed that a phenolic-rich GPE prevents adipocyte hypertrophy in eWAT from rats with metabolic syndrome mitigating insulin resistance and inflammation [25]. The most abundant flavonoids in GPE are the flavan-3-ol (-)-epicatechin (EC) and catechin, and the flavonol quercetin (Q) [25]. We previously observed that these flavonoids protect rats from high fructose-induced adipose insulin resistance through the modulation of inflammation and redox signaling [26, 27]. Recent evidence shows that some phenolic compounds are able to activate the sympathetic nervous system or stimulate

the β-adrenergic receptor [28-30] in part because they share a similar chemical structure with catecholamine [31].

Promoting strategies to attenuate adipose dysfunction through nutritional approaches might be relevant in the fight against diet-induced adiposity. Thus, this study investigated whether GPE could exert protective effects on high-fat diet (HFD)-induced epididymal adipose dysfunction through brown-like cell induction and attenuation of adiposity in rats. The underlying protective action of GPE and its major flavonoids EC and Q on the downstream β-adrenergic receptor was also investigated in 3T3-L1 adipocytes. In order to assess whether GPE could induce brown-like cells in eWAT we used a rat model of cardiovascular disease, the spontaneously hypertensive (SHR) and their control normotensive Wistar–Kyoto (WKY) rat strain fed a HFD. SHR rats present an exacerbation of the sympathetic nervous system [6, 32, 33], which makes them susceptible to the emergence of “beige” cells and a good model to study “browning” pathways. Overall, we observed that GPE promoted brown-like cell formation in WAT and diminished adipose dysfunction.

Materials and methods

2.1. Materials

The Folin-Ciocalteu reagent was purchased from Merck (São Paulo, Brazil). Standards of gallic acid (99%), 3-hydroxytyrosol (≥99.5%), (-)-gallocatechin (≥98%), (-)-gallocatechin gallate (≥99%), (-)-epicatechin gallate (≥98%), (+)-catechin (≥99%), (-)-epicatechin (≥95%), caffeic acid (99%), syringic acid (≥95%), coumaric acid (99%), ferulic acid (≥99%), trans-resveratrol

(≥99%), quercetin hydrate (95%), kaempferol-3-glucoside (≥99%) and malvidin-3-O-glucoside chloride (≥95%) were purchased from Sigma Chemical Co. (St. Louis, MO). The standard of 2-(4-hydroxyphenyl) ethanol (tyrosol) (≥99.5%) was obtained from Fluka (Buchs, Switzerland). MeOH and formic acid were purchased from Mallinckrodt Baker (Inc. Pillispsburg, NJ, USA). Ultrapure water was obtained from a Milli-Q system (Millipore, Billerica, MA, USA). Bovine and porcine fat was from Recreo Refrigerating Industries S.A.I.C. (Santa Fe, Argentina). Commercial kits for the determination of cholesterol, HDL cholesterol, and triglyceride (TG) concentrations were purchased from GTLab (Buenos Aires, Argentina).

The antibody for UCP-1 (U6382) was purchased from Sigma Chemical Co. (St. Louis, MO). The antibody for resistin (AB3371P) was from Millipore, (Billerica, MA, USA). Antibodies for phospho ERK (Tyr204) (sc-7383), ERK (sc-93), PGC-1α (sc-293168), PPARγ (sc-7273), Flk-1 (VEGF-R2) (sc-504), Cluster of differentiation 68 (CD68) (sc-59103), and Nox4 (sc-21860) were obtained from Santa Cruz Biotechnology (Santa Cruz, CA, USA). Antibodies for p38 (#9212), phospho (Thr180/Tyr182) p38 (#9211), AMP kinases (AMPK) (#5832), phospho (Thr172) AMPKα (#2535), adipose triglyceride lipase (ATGL) (#2138) PKA (#9621) and phospho (Thr197) PKA (#4781), SB203580 (p38 inhibitor) and U0126 (ERK inhibitor) were from Cell Signaling Technology (Danvers, MA, USA). PRDM16 (ab106410) was from Abcam (Cambridge, MA, USA) and VEGF-A (MAB293) was from R&D Systems. Nitrocellulose membranes and the Western blotting system were obtained from BIO-RAD (Hercules, CA, USA). Dulbecco's Modified Eagle Medium (DMEM), collagenase type I, TRIzol, M-MLV reverse transcriptase, random primers, Taq polymerase and dNTPs were

obtained from Invitrogen Life Technologies (Carlsbad, CA, USA). Fetal Bovine Serum (FBS) was from PAA Laboratories GmbH (Pasching, Austria). EvaGreen Dye was from Biotium (Fremont, CA, USA). Unless otherwise noted, reagents were purchased from Sigma Chemical Co. (St. Louis, MO, USA).

2.2. Grape pomace extract sampling

GPE was obtained as we previously described [25] from *Vitis vinifera* L. cv. Malbec. Grape pomace (GP) was provided by the Catena Institute of Wine from the Adriana vineyard located in Gualtallary, Mendoza, Argentina. The vinification procedure was conducted with mechanical daily pumping. The skins and seeds were in contact with the juice for 11 days. After that, must was pressed. Fresh GP samples were collected and placed in ice cooled boxes for transportation to the laboratory, and then, stored at -20°C until processing. The GPE was obtained by solid-liquid extraction according to the method of Antoniolli et al. [34]. Five mg of lyophilized GPE was dissolved in 5 mL of ethanol 50% (v/v) aqueous solution for further analysis of the total phenolic content by the Folin–Ciocalteu assay according to Antoniolli et al. [34], and the low molecular weight polyphenols (LMW-PPs) were determined according to Fontana et al. [35].

2.3. Animal study

All procedures were approved by the Institutional Animal Care and Use Committee of the School of Medical Science, University of Cuyo (Protocol approval Nº 36/2014). SHR (n=18) and WKY rats (n=18) at 9 weeks of age were included in this experiment. Rats were housed under controlled conditions

of temperature (23 ± 1ºC) and light (12 h light/12 h dark cycle). Male rats of both strains were randomly divided into three experimental groups (6 rats/group) treated during 10 weeks as follow: A. control (Ctrl) group receiving a standard chow diet; B. a HFD (HF) group containing 40% fat (w/w) (20% bovine and 20% porcine fat) added to the standard chow; and C. HFD group supplemented with 300 mg GPE/Kg body weight (HFGPE). The fat and GPE was incorporated into a pellet mixture as previously reported [25]. Briefly, the corresponding amount of GPE, as lyophilized ground powder, and/or fat was incorporated into the pellet mixture. Pellets were re-made and stored at 4°C. Every two-three days pellets were weighed and dispensed. Body weight was recorded weekly. Food and water intakes were determined three times a week and systolic blood pressure (SBP) was measured at the beginning, 5 and 10 weeks on the protocols by a tail-cuff method using a plethysmography Koda2® (Kent Scientific Corporation, USA). After 10 weeks on the dietary treatments, and after an overnight fast, rats were weighed, anesthetized with ketamine (50 mg/kg body weight) and acepromazine (1 mg/kg body weight), and blood was collected from the abdominal aorta into EDTA-containing tubes. Plasma was obtained after centrifugation at 1,000 x g for 15 min at 4ºC. eWAT was weighed and flash-frozen in liquid nitrogen and then stored at -80ºC until assayed. A piece of eWAT was immediately fixed in 10% (w/v) neutral formalin solution for 24 h and processed for histological analysis.

2.4. Biochemical determinations

Plasma TG, HDL and total cholesterol concentrations were determined by enzymatic colorimetric methods using commercial kits (GTLab, Buenos

Aires, Argentina). Glucose was measure in blood collected from the tail using a glucometer (Accu-Chek Performa, Roche, Buenos Aires, Argentina). Free fatty acids (FFA) were determined using commercial kit (Randox Laboratories, United Kingdom).

2.5. Western blots analysis

Tissue homogenates were prepared as previously described [26, 27]. Aliquots of total homogenates containing 25-40 µg protein were denatured with Laemmli buffer, separated by reducing 8-12.5% (w/v) polyacrylamide gel electrophoresis, and electroblotted onto nitrocellulose membranes. Membranes were blocked for 2 h in 5% (w/v) non-fat milk, and subsequently incubated in the presence of the corresponding primary antibodies (1:1000 dilution) overnight at 4°C. After incubation for 90 min at room temperature in the presence of the corresponding secondary antibody (either HRP or biotinylated antibody followed for 1 hour incubation with streptavidin) the conjugates were visualized and quantified by chemiluminescence detection in a Luminescent Analyzer Image Reader (LAS-4000) Fujifilm. The densitometric analysis was performed using the Image J Program.

2.6. Histological analysis

Adipocyte hypertrophy degree was evaluated in eWAT sections prepared from paraffin-embedded samples and stained with hematoxylin and eosin. Images were analyzed using a CCD camera (Nikon, Japan) 20x magnification and adipocyte area was measure using the Image J program.

2.7. Immunohistochemistry

Paraffin cuts of eWAT were dewaxed and then fixed in a solution of 4% (w/v) paraformaldehyde in phosphate-buffered saline (PBS). After two washes in PBS, samples were incubated with $ClNH_4$ 50 mM under UV light overnight. After one wash for 10 min with PBS, samples were subsequently washed with permeabilizing solution (0.15 Tris-HCl pH 7.6, containing 0.15 M NaCl and 0.1% (w/v) NaN_3) for 30 min. Sections were incubated with an UCP-1 antibody diluted (1:100) in permeabilizing solution, overnight at 4ºC. Samples were subsequently washed three times with PBS for 10 min, and then incubated with the secondary goat anti-rabbit IgG TRITC (Sigma, St. Louis, MO, USA) in permeabilizing solution (diluted 1:750) for 1 h at room temperature. Then, samples were washed with PBS as described above. After drying, sections were covered with an anti-fading solution of Fluoroshield (Sigma-Aldrich, USA). Images were obtained in a Nikon 80i microscope attached to a CCD camera (Nikon, Japan). Three sections per animal (n= 3) were imaged.

2.8. RNA isolation and real-time PCR

RNA was extracted from eWAT using the TRIzol® Reagent according to manufacturer's instructions. mRNA levels of *Vegf-a, Vegf-r2, Tnfα, Mcp-1*, *Pparγ, Prdm16 and Pgc1α* were estimated by real-time RT-PCR technique normalized by *Gapdh* housekeeping gene expression as previously described by Shuman et al. [36] with some modifications. Primers for rat genes were designed as follow: *Tnfα* (forward) 5'-CCACGCTCTTCTGTCTACTG-3', (reverse) 5'-GGCTACGGGCTTGTCACTC-3'; *Pparγ* (forward) 5'-CTGAAGCTCCAAGAATACCA-3', (reverse) 5'-TCCCCACAGACTCGGCACTC-3'; *Mcp-1* (forward) 5'-TGCAGGTCTCTGTCACGCTTC-3', (reverse) 5'-

TTCTCCAGCCGACTCATTGG-3'; *Vegf-a* (forward) 5'-AATGATGAAGCCCTGGAGTG-3', (reverse) 5'-ATGCTGCAGGAAGCTCATCT-3'; *Vegf-r2* (forward) 5'-TAGCAC GACAGAGACTGTGAGG-3', (reverse) 5'-TGAGGTGAGAGAGATGGGTAGG-3'; *Gapdh* (forward) 5'-CTGACATGCCGCCTGGAGAAAC-3', (reverse) 5'-CCA GCATCAAAGGTGGAAGAAT-3'; *Prdm16* (forward) 5'-TTGGTGCAT GTGAAAGAAGG-3', (reverse) 5'-CCTCAGGCTTGAGCTCCTC-3'; *Pgc1α* (forward) 5'-AAAAGCTTGACTGGCGTCAT-3', (reverse) 5'-TCAGGA AGATCTGGGCAAAG-3'.

Briefly, total RNA concentrations were determined spectrophotometrically and RNA integrity was examined by 1% (w/v) agarose gel electrophoresis. First strand cDNA synthesis from 1ug RNA per sample was performed at 37 ºC using Moloney Murine Leukemia Virus Reverse Transcriptase and random hexamer primers in a 12.5 µl reaction mixture. Real-time PCR was performed using a Bio-Rad iQiCycler Detection System (Bio-Rad Laboratories) and Eva-Green™ Dye detection in a final volume of 20 µL. Melt curve analysis was performed after every run to ensure a single amplified product for every reaction. Real Time quantification was monitored by measuring the increase in fluorescence caused by the binding of EvaGreen™ dye to double-strand DNA at the end of each amplification cycle. The authenticity of the amplicons generated was confirmed by their size on a 2% (w/v) agarose gel. In accordance with the literature, we did not find differences among experimental groups in the housekeeping gene expression.

2.9. Adipocyte cell culture and incubations

2.9.1. Stromal vascular fraction isolation

eWAT samples obtained from male WKY and SHR rats fed the control diet were placed in cold PBS and cut into small pieces. Samples were incubated with collagenase type I (1 mg/mL) in a water bath at 37°C for 30 min. After filtration through a 70 µm mesh, preparations were centrifuged at 300 x g for 10 min. Mature adipocytes present in the supernatant were removed and the pellet containing the stromal vascular fraction was washed and plated in DMEM containing 25 mM glucose, 10% (v/v) fetal bovine serum (FBS), 50 U/ml penicillin, and 50 µg/ml streptomycin in an atmosphere of 5% (v/v) CO2 at 37°C. The medium was changed every 3 days until the cell monolayer reached confluence.

2.9.2. Primary adipocyte differentiation and GPE stimulation

Adipocyte differentiation was induced as previously reported [37] with some modifications. Briefly, cells at confluence (day 1) were differentiated by incubation with induction medium (DMEM supplemented with FBS 10% and 10 mmol/L insulin (differentiation medium (DM)) plus 0.5 mmol/L isobutylmethylxanthine, 0.1 mmol/L indomethacin, and 0.25 mmol/L dexamethasone). Two days after induction (day 3), cells were returned to DM, exhibiting at day 8 a fully differentiated phenotype with massive accumulation of multilocular and unilocular fat droplets.

Differentiated adipocytes were treated with or without SB203580 or U0126 for 30 min and incubated with or without GPE (30 µM) for 20 minutes in order to evaluate total and phosphorylated p38 and ERK protein levels (day 8)

or UCP-1 (day 4). A 20 min period of treatment with GPE was chosen based on results of a time course study showing significant activation of p-p38 and p-ERK at this time point **(supplementary Figure 1)**. The amount of GPE used was based on results of a pilot concentration-dependence study showing a significant activation of PGC1-α, PPARγ and UCP-1 at 30 μM of GPE **(data not shown)** and on concentrations reported by Chuang CC. et al. [38] using grape powder extract.

2.9.3. 3T3-L1 adipocytes

3T3-L1 preadipocytes were differentiated as we previously described [27, 37]. Cells were used at day 10 when they presented a fully differentiated phenotype with massive accumulation of fat droplets. Adipocytes were treated with 1 μM EC, 1μM Q or 30 μM GPE and subsequently treated with palmitate (8 mM) for 24 h.

3. Statistical analysis

Data are shown as mean ± SEM. Statistical significances were assessed by one-way ANOVA followed by Newman-Keuls Multiple Comparison Test. GraphPad Prism version 5.00 for Windows (GraphPad Software, San Diego, CA, USA) was used for all statistical analysis. Differences were considered significant at $p<0.05$.

4. Results

4.1. Chemical characterization of GPE

The levels of LMW-PPs and individual anthocyanin content in Malbec GPE are presented in **Table 1 and 2**, respectively. The most abundant flavonoids in the extracts were the flavanols (+)-catechin and EC, the flavonol Q and syringic acid **(Table 1)**. **Table 2** summarizes the GPE individual anthocyanin concentration grouped based on the type of the derivative (non-acylated, acylated, and coumarylated). In terms of concentration, malvidin 3-O-glucoside was the predominant anthocyanin, followed by malvidin 3-O-p-coumaroylglucoside and petunidin 3-O-glucoside. Malvidin and petunidin were the most abundant considering anthocyanin types.

4.2. Effect of GPE supplementation on metabolic parameters in HFD-fed rats

The effect of GPE supplementation on metabolic parameters in WKY and SHR rats fed a HFD are shown in **Table 3**. The average daily food intake was significantly higher in the Ctrl WKY group compared to WKY and SHR rats consuming the HFD. No significantly differences were observed in the daily food intake of WKY supplemented with GPE compared with Ctrl and HF WKY. The energy intake was similar among groups.

As expected, the initial body weight at the beginning of the treatment was significantly higher in WKY rats compared with SHR rats (245±3 and 193±3 g respectively) **(data not shown)**. At the end of the experimental period and after 10 weeks on the HFD body weight was 23% higher in WKY rats compared to Ctrl WKY rats. No differences were observed in body weight among SHR groups. Supplementation with GPE did not modify the body weight in both WKY and SHR strains. HFD consumption led to high plasma TG concentration in

WKY rats, which was partially attenuated by GPE supplementation. HFD consumption partially and significantly increased the levels of plasma FFA in WKY and SHR rats compared to Ctrl WKY rats. GPE supplementation significantly reduced plasma FFA in SHR rats at levels comparable to Ctrl WKY rats, and significantly increased HDL cholesterol levels with respect to both WKY and SHR control rats.

As expected, the SBP was significantly higher in the SHR strain compared with WKY from the beginning of the treatment. HFD consumption did not modify the SBP. However, GPE supplementation significantly reduced SBP in SHR rats from week five on the treatment. Overall, GPE attenuated HFD-induced metabolic alterations, and decreased SPB in SHR rats.

4.3. Effects of GPE supplementation on brown and white adipose weight and adipocyte area in eWAT

The effects of GPE supplementation on BAT and eWAT weight are shown in **Fig. 1A and B**. SHR rats had higher BAT weight upon HFD consumption compared to the WKY strain. GPE supplementation did not modify BAT weight **(Fig. 1A)**. In addition, HFD consumption led to high eWAT weight and adipocyte size in WKY rats, suggestive of hypertrophy **(Fig. 1B-D)**. Supplementation of HFD-fed WKY rats with GPE led to significantly smaller adipocytes without changes in adipose weight, suggestive of hyperplasia. In contrast, the eWAT weight and the diameter of adipocytes of SHR rats were not affected by the addition of fat to the diet.

4.4. Effects of GPE supplementation on inflammatory/oxidative markers and on angiogenesis in eWAT

Next, we explored whether GPE could attenuate HFD-induced adipose immune cell infiltration, inflammation and oxidative damage. HFD consumption caused higher levels of TNFα and MCP-1 mRNA, and protein levels of the macrophage marker CD68 in SHR rats, which was prevented by GPE supplementation **(Fig. 2A and B)**.

Protein levels of resistin, a pro-inflammatory adipocytokine, were higher in WKY HF and in all SHR groups, while those of Nox4 were higher in the WKY/SHR HF groups. GPE supplementation significantly reduced HFD-induced increase of resistin and Nox4 protein in both WKY and SHR strains **(Fig. 2B)**.

To investigated whether GPE could reduce adipocytes diameter in eWAT from WKY rats, we next measured protein and mRNA levels of VEGF-A and its receptor VEGF-R2 which has a central role in angiogenesis. HFD significantly increased VEGF-A protein levels in both strains, while VEGF-R2 was higher only in SHR rats. GPE supplementation significantly enhanced VEGF-A and VEGF-R2 protein levels in WKY compared to WKY HF and Ctrl groups. The VEGF-A mRNA expression was enhanced by GPE in SHR. No differences were observed in VEGF-A and VEGF-R2 mRNA expression among WKY rats **(Fig. 2C and D)**. In addition, PPARγ a key regulator of adipogenesis and adipose metabolism was significantly increased in WKY and SHR by GPE supplementation **(Fig. 3A and B)**. Together, enhanced angiogenesis and adipogenesis could facilitate healthy eWAT expansion, reflected by smaller average size of adipocytes from WKY rats.

4.5. GPE supplementation induces transcriptional regulators of browning in eWAT from SHR rats

In order to explore proteins involved in the appearance of brown-like cells in WAT, proteins and mRNA levels of PGC-1α, PPARγ and PRDM16, and UCP-1 protein levels were measured in eWAT by Western blot and RT-PCR respectively. GPE supplementation significantly increased the protein levels of PPARγ in WKY and significantly increased PGC-1α, PPARγ and PRDM16 in eWAT from SHR **(Fig. 3A)**. The mRNA levels of PGC-1α and PRDM16 were up-regulated in eWAT from Ctrl SHR compared with WKY groups and with HF SHR. GPE significantly increased the mRNA levels of PGC-1α and PPARγ in SHR **(Fig. 3B)**. The UCP-1 protein levels were higher in Ctrl SHR compared with Ctrl and HF WKY, and with HF SHR groups. Supplementation with GPE partially and significantly increased the protein levels of UCP-1 in eWAT from WKY and SHR rats, respectively **(Fig. 3C)**. UCP-1 up-regulation by GPE supplementation in eWAT from SHR rats was confirmed by immunohistochemistry **(Fig. 3D)**.

4.6. GPE stimulates UCP-1 via the p38 and ERK pathways

In primary adipocytes isolated from control SHR rats the addition of 30 μM GPE during the differentiation period enhanced the expression of PGC-1α, PPARγ, PRDM16 and UCP-1 compared to adipocytes derived from control WKY **(data not shown)**.

The p38 and ERK1/2 pathways are involved in the development of beige cells, specially mediated via the β-adrenergic receptor. To elucidate possible mechanisms involved in GPE-mediated UCP-1 protein increase, we first evaluated if GPE affected p38 and ERK1/2 activation. ERK1/2 and p38 phosphorylation was enhanced in adipocytes from SHR rats incubated for 20

min with 30 μM GPE **(supplementary figure 1)**. When adipocytes derived from SHR were incubated with p38 and ERK inhibitors, the protein levels of p-ERK and p-p38 was significantly decreased, in association with a significantly reduced expression of UCP-1, suggesting that p38/ERK is required for UCP-1 activation. No differences were observed in p38, ERK or UCP-1 protein expression in adipocytes from WKY rats **(Fig. 4A and B)**.

4.7. GPE activates the signaling cascade downstream the β-adrenergic receptor in 3T3-L1 adipocytes

Activation of PKA occurs downstream the binding of catecholamine to the β-adrenergic receptor. Taking into account the above results, we next evaluated whether activation of the β-adrenergic pathway is related to GPE-mediated emergence of beige cells. Thus, differentiated 3T3-L1 adipocytes were treated with palmitate without or with GPE, EC and Q, the main phenolic compounds found in GPE. An increase in PKA phosphorylation was observed in adipocytes stimulated with both EC and GPE. In addition, there was a significant increase of AMPK and ERK phosphorylation, and ATGL expression in adipocytes treated with EC, Q and GPE, whereas p38 phosphorylation was only increased by GPE **(Fig. 5A)**. Interestingly, stimulation with EC, Q, and GPE prevented the decrease of proteins involved in mitochondrial biogenesis in 3T3-L1 adipocytes treated with palmitate **(Fig. 5B)**.

5. Discussion

The appearance of brown-like cells in WAT by bioactive compounds constitutes an interesting strategy to mitigate adiposity and metabolic alterations associated to excess energy intake. This study shows that supplementation with GPE, rich in a wide variety of phenolic compounds, stimulates the emergence of brown-like cells in eWAT from SHR rats fed a HFD. This effect can be in part attributed to GPE capacity to stimulate the expression of UCP-1 via p38 and ERK1/2. The downstream activation of the β-adrenergic receptor cascade (PKA, AMPK, ERK, p38, ATGL, PPARγ) by GPE was confirmed in 3T3-L1 adipocytes treated with palmitate.

It has been previously shown that adipose hypertrophy promotes adipose inflammation and/or dysfunction while a reduction of adipocyte diameter even in the absence of adipose tissue mass reduction may prevent these alterations [3]. Accordingly, HFD consumption by WKY rats led to adipocyte hypertrophy accompanied with altered parameters of adipose function, including higher expression of markers of inflammation and oxidative stress, i.e. resistin and Nox4. GPE supplementation mitigated all these events showing that even not modifying eWAT weight, a lower adipocyte diameter is linked to decreased adipose inflammation.

GPE-mediated reduction in the size of adipocytes could be due to enhanced expression of proteins involved in adipogenesis and angiogenesis, such as PPARγ, VEGF-A and its receptor 2. These protein are also associated with brown-like cells induction in WAT depots [5], and could be involved in the slightly augmentation of UCP-1 observed in WKY rats. The effects of phenolic compounds on angiogenesis and adipogenesis in the attenuation of adipose

dysfunction is controversial [39]. Given that angiogenesis supports the expansion of adipose tissue [40], several studies have developed antiangiogenic approaches as a therapeutic intervention for obesity. Administration of angiogenic inhibitors to obese mice results in decreased adipose tissue mass and weight loss [41]. However, other studies argue that inhibition of adipose tissue expansion by changes in angiogenesis can lead to lipotoxicity and metabolic dysfunction due to ectopic fat accumulation [42]. It has been shown that VEGF overexpression in adipose tissue from mice fed a HFD prevents fat mass increase and insulin resistance [5, 7]. On the other hand, obese mice overexpressing adiponectin present high adipose PPARγ expression, reduced adipose macrophage infiltration, and reduced systemic inflammation with normalized metabolic parameters [43].

In spite of SHR rats not showing increased eWAT mass upon HFD consumption, we observed an upregulation of proteins involved in inflammation, i.e.TNFα, resistin, MCP1, CD68, and in oxidant production, i.e. Nox4. These alterations in HFD-fed SHR rats were mitigated upon GPE supplementation. In line with these findings, we recently showed that GPE and polyphenols found in high concentrations in GPE, such as EC, Q and catechin, attenuate inflammation in eWAT from rats fed a high-fructose or/and HFD [25-27, 37, 44]. These effects could be mediated by the capacity of some polyphenols to modulated oxidants production and pro-inflammatory signaling.

Visceral adipose tissue (VAT), and in particular the epididymal fat pad, is less susceptible to browning compared with subcutaneous (inguinal) WAT [45], however several studies have shown the presence of brown-like cells in eWAT

from mice or rats under different experimental conditions [46, 47]. Very importantly, agonists of the β-adrenergic receptor induce the formation of brown-like cells, and the β-adrenergic receptor is most active in VAT (including eWAT) than in other WAT pads [48]. Taking into account that VAT is associated with a higher risk of metabolic diseases, an improvement in VAT biological characteristics may result in a better prognosis of the pathologies associated with excess fat consumption/adiposity. Interestingly, GPE supplementation stimulated the expression of the main transcriptional regulators of brown-like cell development, i.e. PGC-1α, PPARγ, PRDM16 and specifics markers of beige cells i.e. UCP-1 in eWAT from SHR rats exposed to the HFD. This effect can be in part attributed to GPE capacity to activate p38 and ERK1/2 pathways as shown in primary adipose cells from control SHR rats. In contrast to SHR, GPE slightly increase UCP-1 in eWAT from WKY rats. These differences are probably due to the fact that SHR show greater release of interstitial norepinephrine compared with its control strain WKY [49]. In addition, GPE and two of the major GPE flavonoids, EC and Q, enhanced PGC-1α, PPARγ, PRDM16 and UCP-1 expression through the up-regulation of the β-adrenergic receptor downstream cascade in 3T3-L1 adipocytes treated with palmitate.

Brown-like cells could develop in WAT depots through different mechanisms, including differentiation of pre-existing brown adipocyte precursors within WAT [50], differentiation of existing white adipocyte precursors [51], or by trans differentiation from existing white adipocytes [52]. Bioactive compounds such as polyphenols had been recently implicated in the emergence of brown-like cells in WAT [53]. Flavonoids, such as EC or Q,

possess a catechol group with similar chemical structure to catecholamine. This can explain their capacity to activate the β-adrenergic receptor in 3T3-L1 adipocytes treated with palmitate. GPE also increased the activation/expression of proteins downstream the β-adrenergic receptor, i.e. PKA, AMPK, ERK, p38, ATGL, including PGC-1α, PPARγ, PRDM16 and UCP-1 expression. Consistently, an onion peel extract and its main polyphenol compound, Q, promote brown-like adipocyte appearance in mouse WAT and in 3T3-L1 cells [54]. This was in part attributed to the activation of AMPK [54]. Catechins present in green tea stimulate energy expenditure and/or thermogenesis [28, 55]. Moreover, dihydromyricetin, from a Rattan tea extract, increases serum irisin secretion both *in vitro* and *in vivo*, which occurred in part via the PGC-1α signaling pathway [29]. A flavan-3-ol fraction derived from cocoa, rich in EC and catechin, increases the energy expenditure associated with enhanced catecholamine secretion [30]. Overall, the above evidence supports the involvement of the β-adrenergic receptor in the fat browning effects of GPE, Q and EC. While the interaction of phenolic compounds with different receptors has been described [24], this has not been investigated for the β-adrenergic receptor. Thus, further studies are needed to assess both, the interactions of Q, EC, and other GPE phenolics with the receptor, and/or the existence of other potential mechanisms of activation by Q/EC/GPE of proteins/events downstream the β- adrenergic receptor.

In conclusion, results from this study indicate that GPE increases the expression of the main transcriptional regulators of brown-like cell development, i.e. PGC-1α, PPARγ, PRDM16 and specifics markers of beige cells i.e. UCP-1 in eWAT from SHR rats and in 3T3-L1 adipocytes. Results support the concept

that this occurs in part through: i) the activation of the β-adrenergic receptor signaling; pathway, and (ii) the promotion of healthy eWAT expansion, suggested by a smaller average size of adipocytes in WKY rats and concomitant reduction of inflammatory markers in eWAT from both WKY and SHR rats. An increased consumption of diets rich in GPE flavonoids may exert positive effects on the quality and quantity of WAT in obese individuals or in those consuming Western-style diets.

Funding

This work was supported by the Universidad Nacional de Cuyo [Programa I+D 2015], Consejo Nacional de Investigaciones Científicas y Tecnológicas (CONICET) [PIP-35686], Agencia Nacional de Promoción Científica y Tecnológica [PICT 2014-0547], PICT 2013-0414 and PICT 2013-1856], and NIFA-USDA (CA-D*-xxx-7244-H) (P.O.).

Table 1. Concentrations of LMW-PPs in freeze-dried Malbec GPE

Analyte	**Concentration (μg g^{-1} GPE)**
Hydroxybenzoic acids	
Gallic acid	253±11
Syringic acid	1732±90
Total	**1985**
Hydroxycinnamic acids	
Caftaric acid	n.d.
Cafeic acid	16±1
p-coumaric acid	65±3
Ferulic acid	24±1
Total	**105**
Stilbene	
Polydatin	12±2
Piceatannol	39±3
trans-resveratrol	36±3
Total	**87**
Flavanols	
(+)-catechin	3387±216
(-)-epicatechin	1763±128
(-)-gallocatechin	n.d.
(-)-epigallocatechin	n.d.
(-)-epigallocatechin gallate	n.d.
Total	**5150**
Flavonols	
Quercetin-3-glucoside	112±7
Kaempferol-3-glucoside	n.d.
Quercetin	557±48
Total	**669**
Other compounds	
OH-tyrosol	n.d.
Tyrosol	34±2
Total	**34**
Total LMW-PPs	**8030**
TPC	**195±30**

Values are shown as means ± SEM, n=3 replicates. n.d., not detected.

Table 2. Concentrations of individual anthocyanins in freeze-dried Malbec GPE

Anthocyanins	**Concentration (µg g^{-1} GPE)**
Delphinidin 3-O-glucoside	4581±412
Cyanidin 3-O-glucoside	870±104
Petunidin 3-O-glucoside	6880±481
Peonidin 3-O-glucoside	2460±248
Malvidin 3-O-glucoside	26658±1866
Total glucosylated	**41449**
Delphinidin 3-O-acetylglucoside	1043±115
Petunidin 3-O-acetylglucoside	1424±152
Peonidin 3-O-acetylglucoside	1902±215
Malvidin 3-O-acetylglucoside	4021±322
Total acetylated	**8391**
Cyanidin 3-O-p-coumaroylglucoside	1886±151
Petunidin 3-O-p-coumaroylglucoside	2481±199
Peonidin 3-O-p-coumaroylglucoside	1854±204
Malvidin 3-O-p-coumaroylglucoside	12864±772
Total coumaroylated	**19085**
Total anthocyanins	**68924**

Average contents (µg g^{-1} GPE) with their standard deviations, n=3 replicates.

Table 3. Effects of GPE on metabolic parameters

	WKY			SHR		
	Ctrl	**HF**	**HFGPE**	**Ctrl**	**HF**	**HFGPE**
Food intake (g/d)	20±1[a]	14 ± 2[b]	16 ± 1[a,b]	17 ± 2[a,b]	12 ± 1[b]	13 ± 1[b]
Energy intake (kcal/d)	51±12	62 ± 17	73 ± 19	47 ± 12	56 ± 15	59 ± 15
Body weight (g)	342 ±16[a]	422 ± 7[b]	417 ± 11[b]	295 ± 4[c]	300 ± 7[c]	285 ± 7[c]
Glucose (mg/dL)	77±4	77 ± 6	92 ± 6	73 ± 1	75 ± 3	74 ± 5
TG (mg/dL)	103 ± 10[a]	131 ± 3[b]	124 ± 2[a,b]	114 ± 4[a,b]	126 ± 6[a,b]	112 ± 2[a,b]
Cholesterol (mg/dL)	72 ± 5	88 ± 4	85 ± 7	69 ± 6	72 ± 3	72 ± 4
HDL (mg/dL)	43,8±2.4[a]	37.7±3.4[a,b]	43.8±2.8[a]	36.5±2[a,b]	32.0±1.3[b]	60.5±1.8[c]
FFA (mmol/L)	0.83 ± 0.07[a]	1.17 ± 0.04[a,b]	0.87 ±0.09[a]	1.22±0.11[a,b]	1.42±0.10[b]	0.83 ± 0.12[a]
SBP mmHg						
0 week	121 ± 1[a]	124 ± 3[a]	122 ± 2[a]	155 ± 2[b]	154 ± 1[b]	156 ± 3[b]
5 weeks	130 ± 1[a]	124 ± 2[a]	128 ± 3[a]	157 ± 3[b]	163 ± 2[b]	151 ± 3[c]
10 weeks	132 ± 2[a]	138 ± 2[a]	133 ± 2[a]	169 ± 3[b]	170 ± 3[b]	159 ± 1[c]

Metabolic parameters from rats fed for 10 weeks without (Ctrl) or with HFD (HF), and HFD supplemented with 300mg GPE/Kg body weight (HFGPE). Values are shown as means ± SEM of six animals/treatment. Values having different superscripts are significantly different ($p<0.05$, one way ANOVA).

Figure legends

Figure 1. Effect of dietary GPE supplementation on brown and white adiposity in rats fed a HFD. (A) BAT and (B) eWAT weight, (C) representative histological images of eWAT stained with hematoxylin and eosin, and (D) mean adipocyte diameter from WKY and SHR rats fed a control diet (Ctrl), a HFD supplemented with 40% fat (HF), or the HFD supplemented with GPE (300 mg Kg/ body weight/d) (HFGPE). Results are shown as mean ± SEM of 6 animals/treatments. Values having different superscripts are significantly different, $p<0.05$, one-way ANOVA test.

Figure 2. Effect of GPE supplementation on inflammatory/oxidative markers and on proteins involved in angiogenesis in eWAT from rats fed a HFD. (A) TNFα and MCP-1 mRNA determined by real-time PCR and normalized by GAPDH expression, (B) CD68, resistin and Nox4 protein expression measured by Western blot, (C) VEGF-A and VEGF-R2 protein levels measured by Western blot, and (D) VEGF-A and VEGF-R2 mRNA levels determined by real-time PCR in eWAT from WKY and SHR rats fed a control diet (Ctrl), a HFD supplemented with 40% fat (HF), or the HFD supplemented with GPE (300 mg Kg/ body weight/d) (HFGPE). Results are shown as mean ± SEM of 3-4 animals/treatment. Bands were quantified and results were expressed as relative to either A and D- β-actin or B and C- GAPDH levels. Values having different superscripts are significantly different, $p<0.05$, one-way ANOVA test.

Figure 3. Dietary GPE supplementation enhances the expression of transcriptional regulators of browning and UCP-1 in eWAT from SHR rats fed a HFD. (A) PGC-1α, PPARγ and PRDM16 protein levels measured by Western blot, (B) PGC-1α, PPARγ and PRDM16 mRNA levels, (C) UCP-1 protein levels measured by Western blot, and (D) UCP-1 levels measured by immunofluorescence in eWAT from WKY and SHR rats fed a control diet (Ctrl), a HFD supplemented with 40% fat (HF), or the HFD supplemented with GPE (300 mg Kg/ body weight/d) (HFGPE). Results are shown as mean ± SEM of 3-4 animals/treatments. Bands were quantified and results were expressed as relative to either A and C- β-actin, B- GAPDH levels and C- Fluorescence intensity was quantified. Values having different superscripts are significantly different, $p<0.05$, one-way ANOVA test.

Figure 4. p38 and ERK are involved in GPE-induced UCP-1 expression in adipocytes from SHR. (A) Phosphorylated and total ERK and p38, and (B) protein levels of UCP-1 were evaluated by Western blot in primary rat adipocytes from WKY and SHR rats. Differentiated adipocytes were pre-treated with SB203580 (p38 inhibitor) or U0126 (ERK inhibitor) (10 mmol/L) for 30 min, and then supplemented with GPE (30 μM) for further 4 days. Results are shown as mean ± SEM of 3-4 independent experiments. Bands were quantified and results were expressed as either the ratio of phosphorylated/total protein levels or relative to β-actin content. Values having different superscripts are significantly different, $p<0.05$, one-way ANOVA test.

Figure 5. GPE and its mayor phenolic compounds promotes the activation of the β-adrenergic downstream cascade in 3T3-L1 adipocytes. (A) Levels of phosphorylated and total PKA, AMPK, ERK, p38 and total ATGL, and (B) PGC1α, PPARγ, PRDM16 and UCP-1 were evaluated in 3T3-L1 adipocytes incubated without or with GPE (30 μM), EC (1μM) and Q (1μM), and subsequently in the absence or presence of 8 mM palmitate for further 24 h. Results were expressed as the ratio of phosphorylated/total or relative to β-actin protein levels. Data represent means ± SEM of 3 independent experiments. Values having different superscripts are significantly different, $p<0.05$, one-way ANOVA test.

References

[1] Despres JP, Lemieux I. Abdominal obesity and metabolic syndrome. Nature 2006 Dec 14;444(7121):881-7.
[2] Jo J, Gavrilova O, Pack S, Jou W, Mullen S, Sumner AE, et al. Hypertrophy and/or Hyperplasia: Dynamics of Adipose Tissue Growth. PLoS Comput Biol 5(3):e1000324 2009.
[3] Kalupahana NS, Moustaid-Moussa N, Claycombe KJ. Immunity as a link between obesity and insulin resistance. Mol Aspects Med. 2012;33:26-34.
[4] van Greevenbroek MM, Schalkwijk CG, Stehouwer CD. Dysfunctional adipose tissue and low-grade inflammation in the management of the metabolic syndrome: current practices and future advances. F1000Res 2016 Oct 13;5 pii: F1000 Faculty Rev-2515 eCollection 2016.
[5] Elias I, Franckhauser S, Bosch F. New insights into adipose tissue VEGF-A actions in the control of obesity and insulin resistance. Adipocyte. 2013;2:109-12.
[6] Hojna S, Jordan MD, Kollias H, Pausova Z. High-fat diet induces emergence of brown-like adipocytes in white adipose tissue of spontaneously hypertensive rats. Hypertens Res;35(3):279-86 2012.
[7] Elias I, Franckhauser S, Ferre T, Vila L, Tafuro S, Munoz S, et al. Adipose tissue overexpression of vascular endothelial growth factor protects against diet-induced obesity and insulin resistance. Diabetes. 2012;61:1801-13.
[8] Jankovic A, Golic I, Markelic M, Stancic A, Otasevic V, Buzadzic B, et al. Two key temporally distinguishable molecular and cellular components of white adipose tissue browning during cold acclimation. J Physiol 2015 Aug 1;593(15):3267-80 doi: 101113/JP270805 Epub 2015 Jul 14.
[9] Gross B, Pawlak M, Lefebvre P, Staels B. PPARs in obesity-induced T2DM, dyslipidaemia and NAFLD. Nat Rev Endocrinol. 2017;13:36-49.
[10] Bjorndal B, Burri L, Staalesen V, Skorve J, Berge RK. Different adipose depots: their role in the development of metabolic syndrome and mitochondrial response to hypolipidemic agents. J Obes. 2011;490650:15.
[11] Echtay KS. Mitochondrial uncoupling proteins--what is their physiological role? Free Radic Biol Med. 2007;43:1351-71.
[12] Kopecky J, Clarke G, Enerback S, Spiegelman B, Kozak LP. Expression of the mitochondrial uncoupling protein gene from the aP2 gene promoter prevents genetic obesity. J Clin Invest. 1995;96:2914-23.
[13] Choi S, Snider AJ. Sphingolipids in High Fat Diet and Obesity-Related Diseases. Mediators Inflamm 2015;2015:520618 doi: 101155/2015/520618 Epub 2015 Nov 16.
[14] Ghorbani M, Claus TH, Himms-Hagen J. Hypertrophy of brown adipocytes in brown and white adipose tissues and reversal of diet-induced obesity in rats treated with a beta3-adrenoceptor agonist. Biochem Pharmacol. 1997;54:121-31.
[15] Vegiopoulos A, Muller-Decker K, Strzoda D, Schmitt I, Chichelnitskiy E, Ostertag A, et al. Cyclooxygenase-2 controls energy homeostasis in mice by de novo recruitment of brown adipocytes. Science. 2010;328:1158-61.
[16] Koh YJ, Park BH, Park JH, Han J, Lee IK, Park JW, et al. Activation of PPAR gamma induces profound multilocularization of adipocytes in adult mouse white adipose tissues. Exp Mol Med. 2009;41:880-95.
[17] Bonet ML, Oliver P, Palou A. Pharmacological and nutritional agents promoting browning of white adipose tissue. Biochim Biophys Acta. 2013;5:969-85.
[18] Bordicchia M, Liu D, Amri EZ, Ailhaud G, Dessi-Fulgheri P, Zhang C, et al. Cardiac natriuretic peptides act via p38 MAPK to induce the brown fat thermogenic program in mouse and human adipocytes. J Clin Invest. 2012;122:1022-36.
[19] Ravussin E, Kozak LP. Have we entered the brown adipose tissue renaissance? Obes Rev 2009 May;10(3):265-8 doi: 101111/j1467-789X200800559x Epub 2009 Jan 19.

[20] Pereira MP, Ferreira LAA, da Silva FHS, Christoffolete MA, Metsios GS, Chaves VE, et al. A low-protein, high-carbohydrate diet increases browning in perirenal adipose tissue but not in inguinal adipose tissue. Nutrition. 2017;42:37-45.
[21] Chiva-Blanch G, Urpi-Sarda M, Ros E, Valderas-Martinez P, Casas R, Arranz S, et al. Effects of red wine polyphenols and alcohol on glucose metabolism and the lipid profile: a randomized clinical trial. Clin Nutr 32(2):200-6 doi: 101016/jclnu201208022. 2013.
[22] Davison K, Coates AM, Buckley JD, Howe PR. Effect of cocoa flavanols and exercise on cardiometabolic risk factors in overweight and obese subjects. Int J Obes (Lond) 2008 Aug;32(8):1289-96 doi: 101038/ijo200866 Epub 2008 May 27.
[23] Dong J, Zhang X, Zhang L, Bian HX, Xu N, Bao B, et al. Quercetin reduces obesity-associated ATM infiltration and inflammation in mice: a mechanism including AMPKalpha1/SIRT1. J Lipid Res 2014 Mar;55(3):363-74 doi: 101194/jlrM038786 Epub 2014 Jan 24.
[24] Fraga CG, Galleano M, Verstraeten SV, Oteiza PI. Basic biochemical mechanisms behind the health benefits of polyphenols. Mol Aspects Med 31(6):435-45 2010.
[25] Rodriguez Lanzi C, Perdicaro DJ, Antoniolli A, Fontana AR, Miatello RM, Bottini R, et al. Grape pomace and grape pomace extract improve insulin signaling in high-fat-fructose fed rat-induced metabolic syndrome. Food Funct 16;7(3):1544-53. 2016.
[26] Bettaieb A, Vazquez Prieto MA, Rodriguez Lanzi C, Miatello RM, Haj FG, Fraga CG, et al. (-)-Epicatechin mitigates high-fructose-associated insulin resistance by modulating redox signaling and endoplasmic reticulum stress. Free Radic Biol Med ;72:247-56. 2014.
[27] Vazquez Prieto MA, Bettaieb A, Rodriguez Lanzi C, Soto VC, Perdicaro DJ, Galmarini CR, et al. Catechin and quercetin attenuate adipose inflammation in fructose-fed rats and 3T3-L1 adipocytes. Mol Nutr Food Res ;59(4):622-33 2015.
[28] Rains TM, Agarwal S, Maki KC. Antiobesity effects of green tea catechins: a mechanistic review. J Nutr Biochem. 2011;22:1-7.
[29] Zhou Q, Chen K, Liu P, Gao Y, Zou D, Deng H, et al. Dihydromyricetin stimulates irisin secretion partially via the PGC-1alpha pathway. Mol Cell Endocrinol. 2015;412:349-57.
[30] Matsumura Y, Nakagawa Y, Mikome K, Yamamoto H, Osakabe N. Enhancement of energy expenditure following a single oral dose of flavan-3-ols associated with an increase in catecholamine secretion. PLoS One. 2014;9.
[31] Fernandez-Fernandez L, Esteban G, Giralt M, Valente T, Bolea I, Sole M, et al. Catecholaminergic and cholinergic systems of mouse brain are modulated by LMN diet, rich in theobromine, polyphenols and polyunsaturated fatty acids. Food Funct 2015 Apr;6(4):1251-60 doi: 101039/c5fo00052a.
[32] Cabassi A, Bergamaschi E, Mutti A, Franchini I, Borghetti A. Age-related changes in interstitial norepinephrine. A microdialysis study in spontaneously hypertensive rats. Am J Hypertens 1996 Sep;9(9):878-83. 1996.
[33] Bosse JD, Lin HY, Sloan C, Zhang QJ, Abel ED, Pereira TJ, et al. A low-carbohydrate/high-fat diet reduces blood pressure in spontaneously hypertensive rats without deleterious changes in insulin resistance. Am J Physiol Heart Circ Physiol 2013 Jun 15;304(12):H1733-42 doi: 101152/ajpheart006312012 Epub 2013 Apr 19.
[34] Antoniolli A, Fontana AR, Piccoli P, Bottini R. Characterization of polyphenols and evaluation of antioxidant capacity in grape pomace of the cv. Malbec. Food Chem. 2015;178:172-8.
[35] Fontana AR, Antoniolli A, Bottini R. Development of a high-performance liquid chromatography method based on a core-shell column approach for the rapid determination of multiclass polyphenols in grape pomaces. Food Chem. 2016;192:1-8.
[36] Schuman ML, Peres Diaz LS, Landa MS, Toblli JE, Cao G, Alvarez AL, et al. Thyrotropin-releasing hormone overexpression induces structural changes of the left ventricle in the normal rat heart. Am J Physiol Heart Circ Physiol. 2014;307:3.

[37] Vazquez-Prieto MA, Bettaieb A, Haj FG, Fraga CG, Oteiza PI. (-)-Epicatechin prevents TNFalpha-induced activation of signaling cascades involved in inflammation and insulin sensitivity in 3T3-L1 adipocytes. Arch Biochem Biophys 15;527(2):113-8 2012.
[38] Chuang CC, Bumrungpert A, Kennedy A, Overman A, West T, Dawson B, et al. Grape powder extract attenuates tumor necrosis factor alpha-mediated inflammation and insulin resistance in primary cultures of human adipocytes. J Nutr Biochem. 2011;22:89-94.
[39] Sun K, Wernstedt Asterholm I, Kusminski CM, Bueno AC, Wang ZV, Pollard JW, et al. Dichotomous effects of VEGF-A on adipose tissue dysfunction. Proc Natl Acad Sci U S A. 2012;109:5874-9.
[40] Cao Y. Angiogenesis modulates adipogenesis and obesity. J Clin Invest. 2007;117:2362-8.
[41] Nishimura S, Manabe I, Nagasaki M, Hosoya Y, Yamashita H, Fujita H, et al. Adipogenesis in obesity requires close interplay between differentiating adipocytes, stromal cells, and blood vessels. Diabetes. 2007;56:1517-26.
[42] Lemoine AY, Ledoux S, Queguiner I, Calderari S, Mechler C, Msika S, et al. Link between adipose tissue angiogenesis and fat accumulation in severely obese subjects. J Clin Endocrinol Metab. 2012;97:2011-649.
[43] Kim JY, van de Wall E, Laplante M, Azzara A, Trujillo ME, Hofmann SM, et al. Obesity-associated improvements in metabolic profile through expansion of adipose tissue. J Clin Invest. 2007;117:2621-37.
[44] Galleano M, Calabro V, Prince PD, Litterio MC, Piotrkowski B, Vazquez-Prieto MA, et al. Flavonoids and metabolic syndrome. Ann N Y Acad Sci1259:87-94. 2012.
[45] Walden TB, Hansen IR, Timmons JA, Cannon B, Nedergaard J. Recruited vs. nonrecruited molecular signatures of brown, "brite," and white adipose tissues. Am J Physiol Endocrinol Metab. 2012;302:9.
[46] Shen W, Chuang CC, Martinez K, Reid T, Brown JM, Xi L, et al. Conjugated linoleic acid reduces adiposity and increases markers of browning and inflammation in white adipose tissue of mice. J Lipid Res 2013 Apr;54(4):909-22 doi: 101194/jlrM030924 Epub 2013 Feb 11.
[47] Lee YH, Petkova AP, Mottillo EP, Granneman JG. In vivo identification of bipotential adipocyte progenitors recruited by beta3-adrenoceptor activation and high-fat feeding. Cell Metab 2012 Apr 4;15(4):480-91 doi: 101016/jcmet201203009.
[48] Arner P. Differences in lipolysis between human subcutaneous and omental adipose tissues. Ann Med 1995 Aug;27(4):435-8.
[49] Cabassi A, Vinci S, Cantoni AM, Quartieri F, Moschini L, Cavazzini S, et al. Sympathetic activation in adipose tissue and skeletal muscle of hypertensive rats. Hypertension. 2002;39:656-61.
[50] Petrovic N, Walden TB, Shabalina IG, Timmons JA, Cannon B, Nedergaard J. Chronic peroxisome proliferator-activated receptor gamma (PPARgamma) activation of epididymally derived white adipocyte cultures reveals a population of thermogenically competent, UCP1-containing adipocytes molecularly distinct from classic brown adipocytes. J Biol Chem. 2010;285:7153-64.
[51] Elabd C, Chiellini C, Carmona M, Galitzky J, Cochet O, Petersen R, et al. Human multipotent adipose-derived stem cells differentiate into functional brown adipocytes. Stem Cells. 2009;27:2753-60.
[52] Cinti S. Transdifferentiation properties of adipocytes in the adipose organ. Am J Physiol Endocrinol Metab. 2009;297:19.
[53] Arias N, Pico C, Teresa Macarulla M, Oliver P, Miranda J, Palou A, et al. A combination of resveratrol and quercetin induces browning in white adipose tissue of rats fed an obesogenic diet. Obesity. 2017;25:111-21.
[54] Lee SG, Parks JS, Kang HW. Quercetin, a functional compound of onion peel, remodels white adipocytes to brown-like adipocytes. J Nutr Biochem. 2017;42:62-71.

[55] Dulloo AG, Seydoux J, Girardier L, Chantre P, Vandermander J. Green tea and thermogenesis: interactions between catechin-polyphenols, caffeine and sympathetic activity. Int J Obes Relat Metab Disord. 2000;24:252-8.

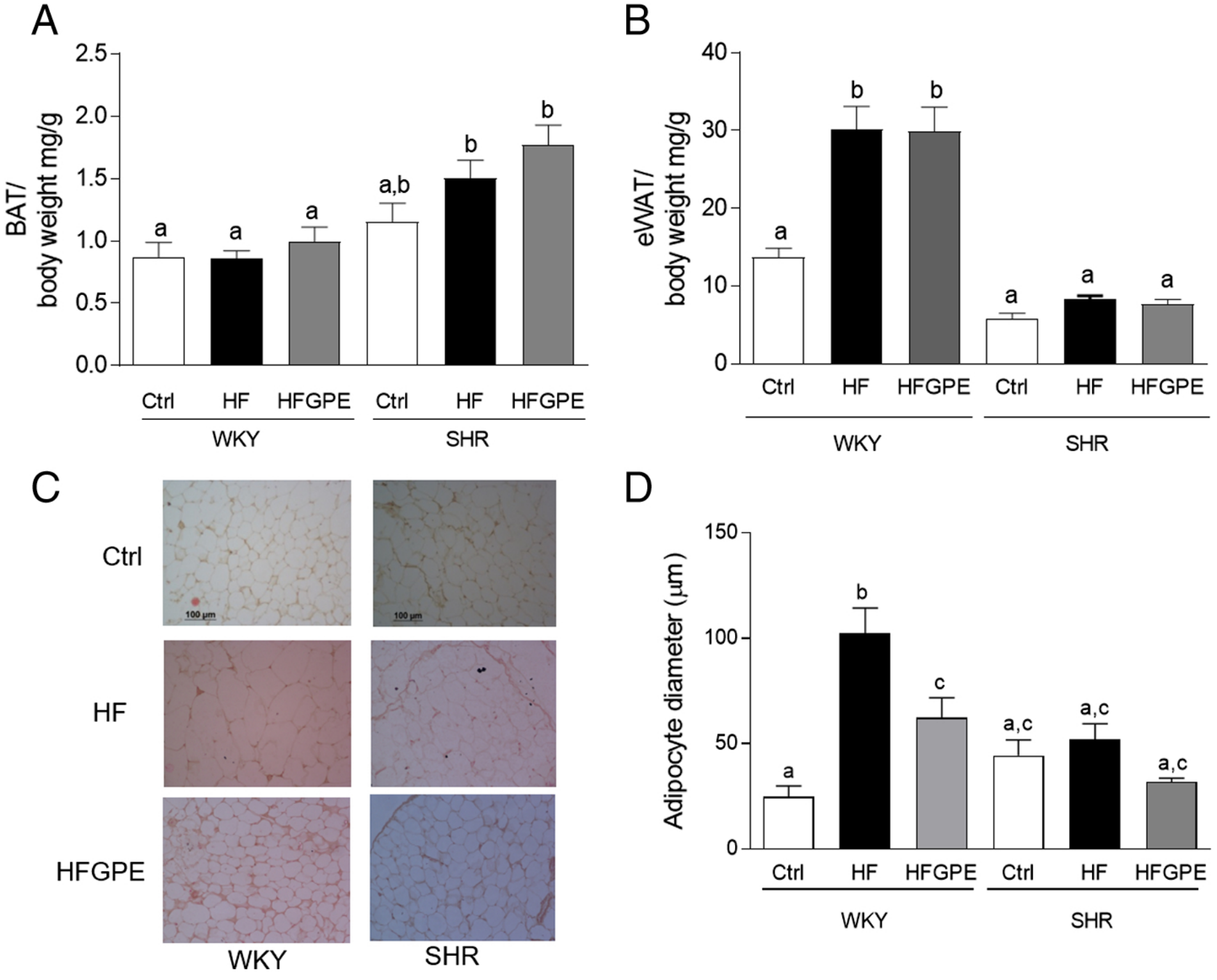
A
BAT/
body weight mg/g
2.5
2.0
1.5
1.0
0.5
0.0
a
a
a
a,b
b
b
Ctrl
HF
HFGPE
Ctrl
HF
HFGPE
WKY
SHR
B
eWAT/
body weight mg/g
40
30
20
10
0
a
b
b
a
a
a
Ctrl
HF
HFGPE
Ctrl
HF
HFGPE
WKY
SHR
C
Ctrl
HF
HFGPE
100 µm
100 µm
WKY
SHR
D
Adipocyte diameter (µm)
150
100
50
0
a
b
c
a,c
a,c
a,c
Ctrl
HF
HFGPE
Ctrl
HF
HFGPE
WKY
SHR

Figure 1

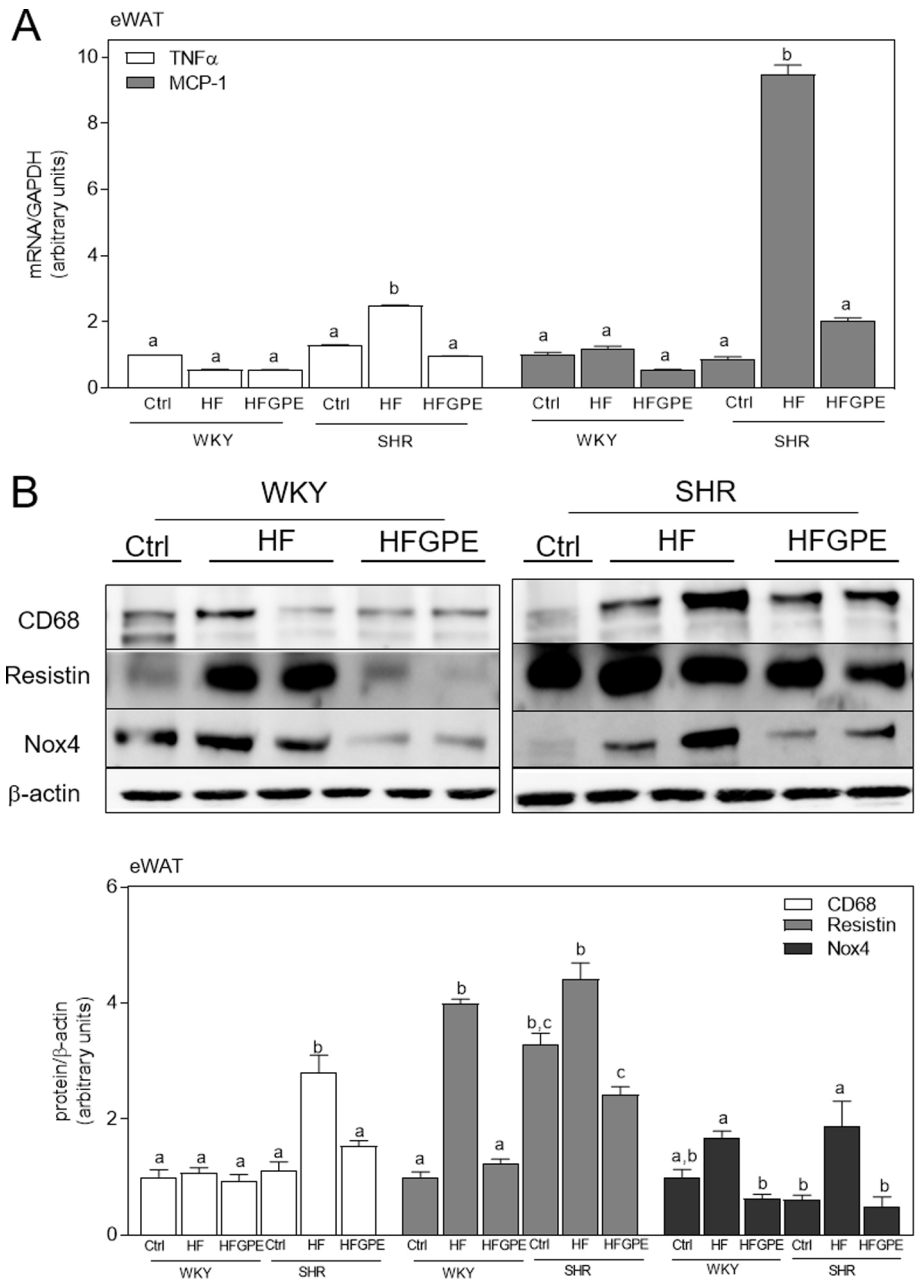
A
eWAT
TNFα
MCP-1
mRNA/GAPDH (arbitrary units)
Ctrl
HF
HFGPE
WKY
SHR
B
WKY
SHR
CD68
Resistin
Nox4
β-actin
eWAT
CD68
Resistin
Nox4
protein/β-actin (arbitrary units)

Figure 2

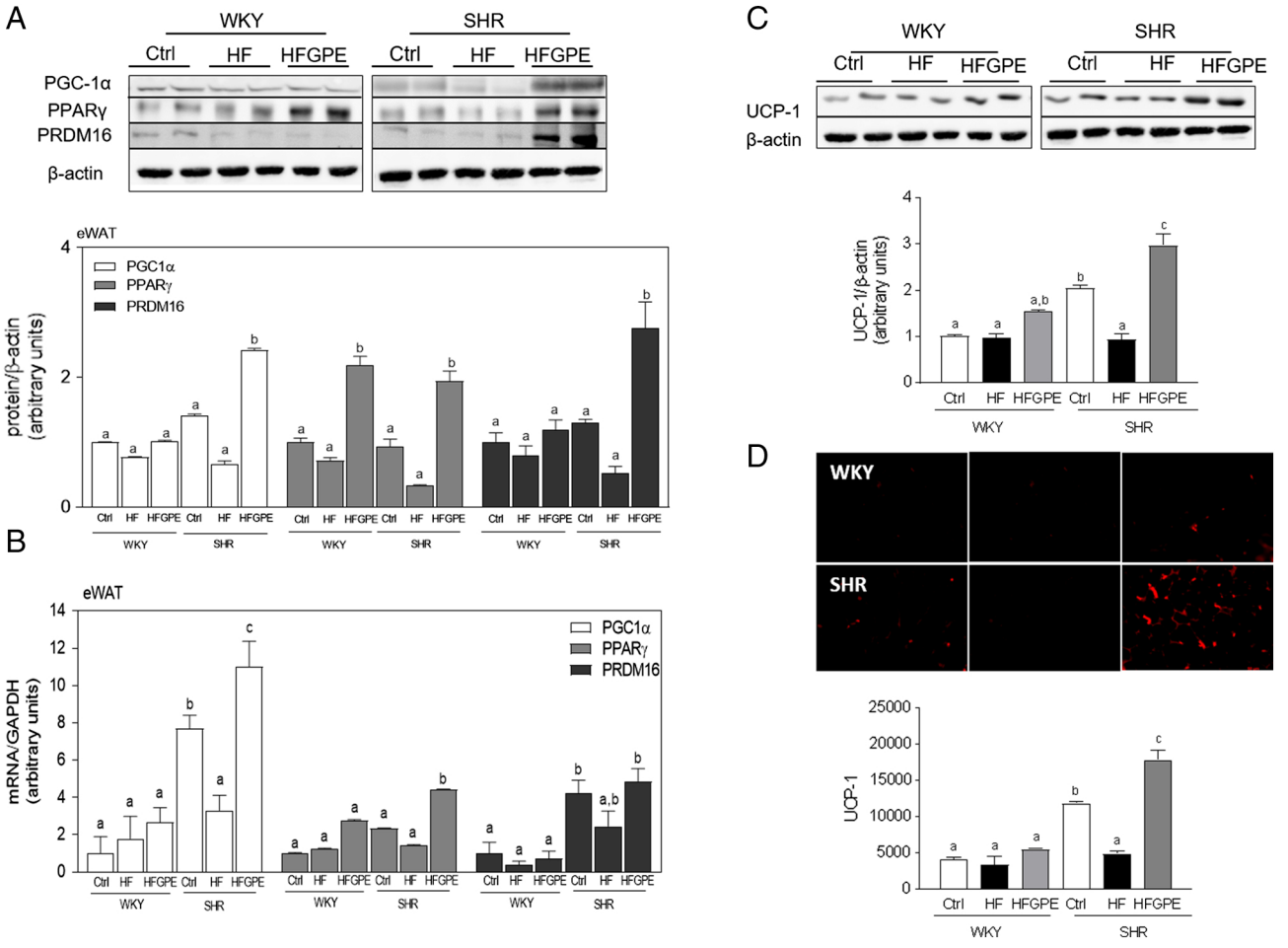
A
WKY
SHR
Ctrl
HF
HFGPE
PGC-1α
PPARγ
PRDM16
β-actin
eWAT
PGC1α
PPARγ
PRDM16
protein/β-actin (arbitrary units)
B
eWAT
mRNA/GAPDH (arbitrary units)
C
UCP-1
β-actin
UCP-1/β-actin (arbitrary units)
D
WKY
SHR
UCP-1

Figure 3

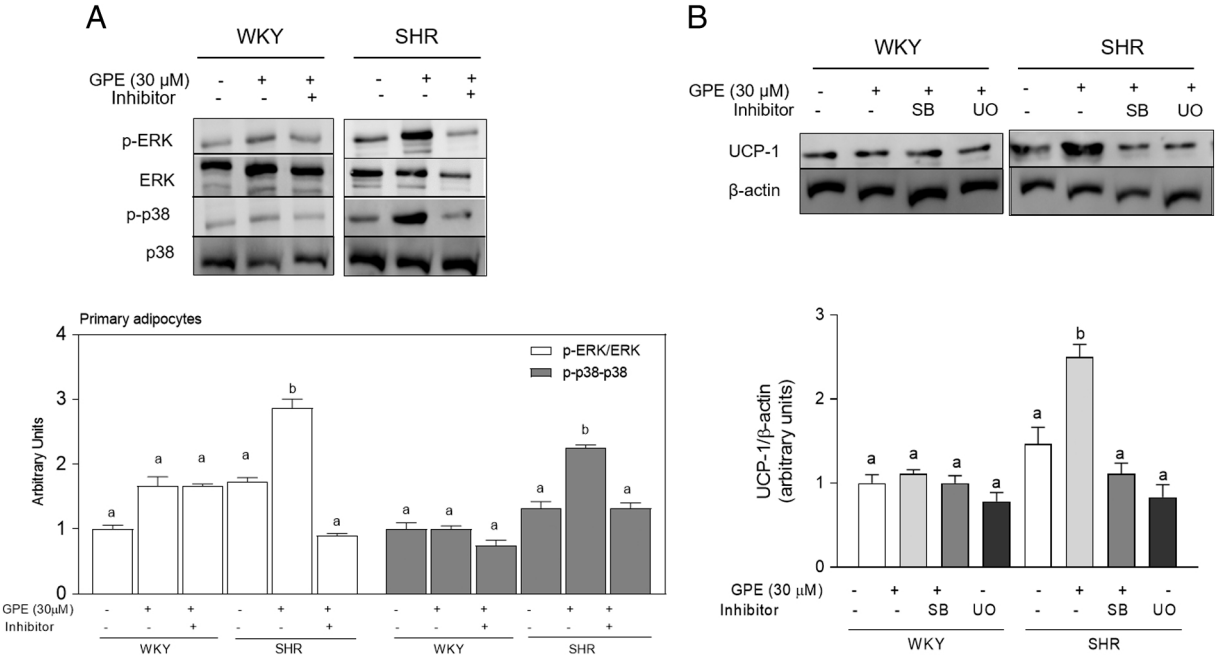
A
WKY
SHR
GPE (30 μM)
Inhibitor
p-ERK
ERK
p-p38
p38
Primary adipocytes
p-ERK/ERK
p-p38-p38
Arbitrary Units
GPE (30μM)
Inhibitor
WKY
SHR
B
UCP-1
β-actin
SB
UO
UCP-1/β-actin (arbitrary units)

Figure 4

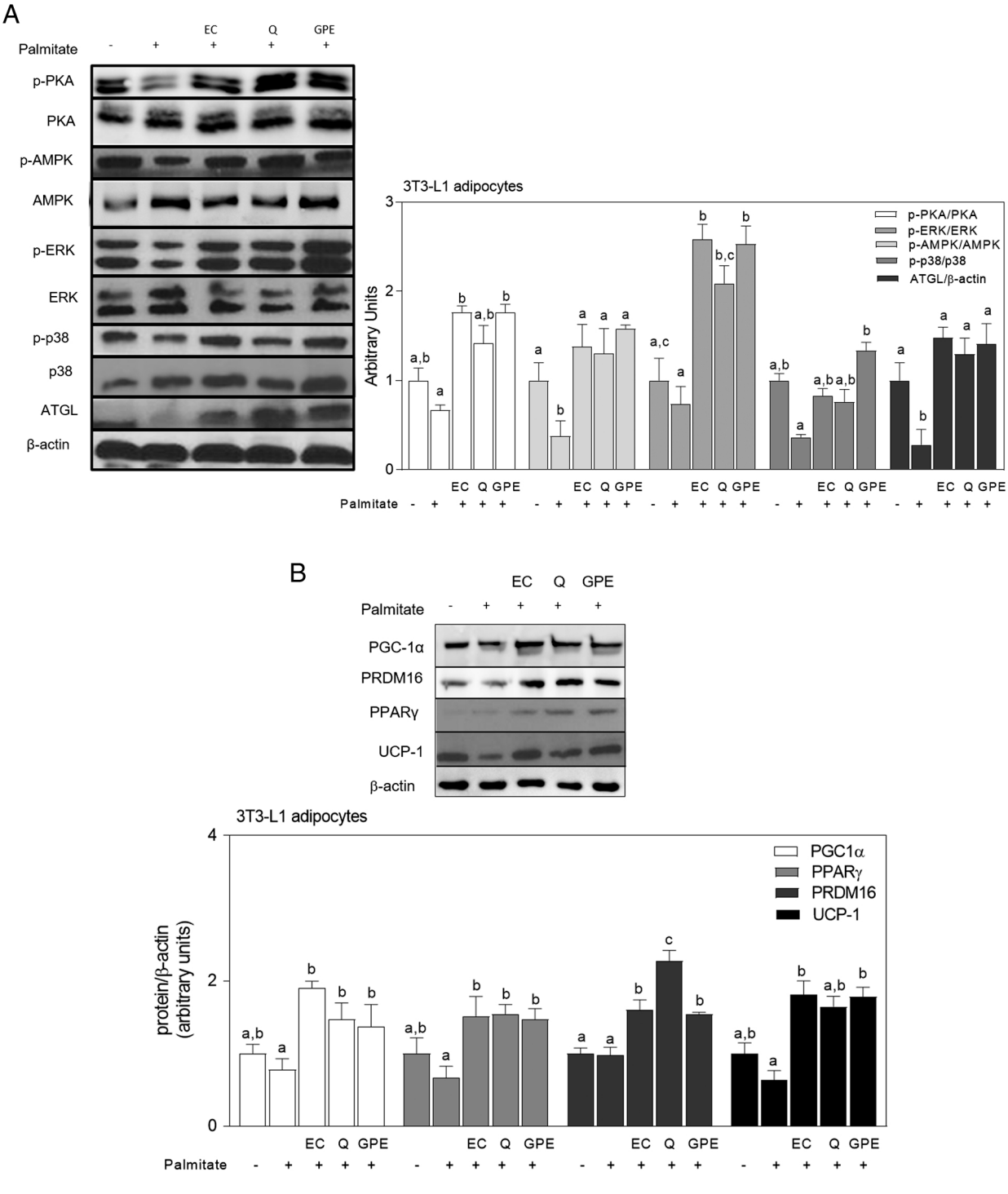
A
Palmitate - + EC + Q + GPE +
p-PKA
PKA
p-AMPK
AMPK
p-ERK
ERK
p-p38
p38
ATGL
β-actin
3T3-L1 adipocytes
Arbitrary Units
p-PKA/PKA
p-ERK/ERK
p-AMPK/AMPK
p-p38/p38
ATGL/β-actin
EC Q GPE
Palmitate
B
PGC-1α
PRDM16
PPARγ
UCP-1
β-actin
3T3-L1 adipocytes
protein/β-actin (arbitrary units)
PGC1α
PPARγ
PRDM16
UCP-1

Figure 5

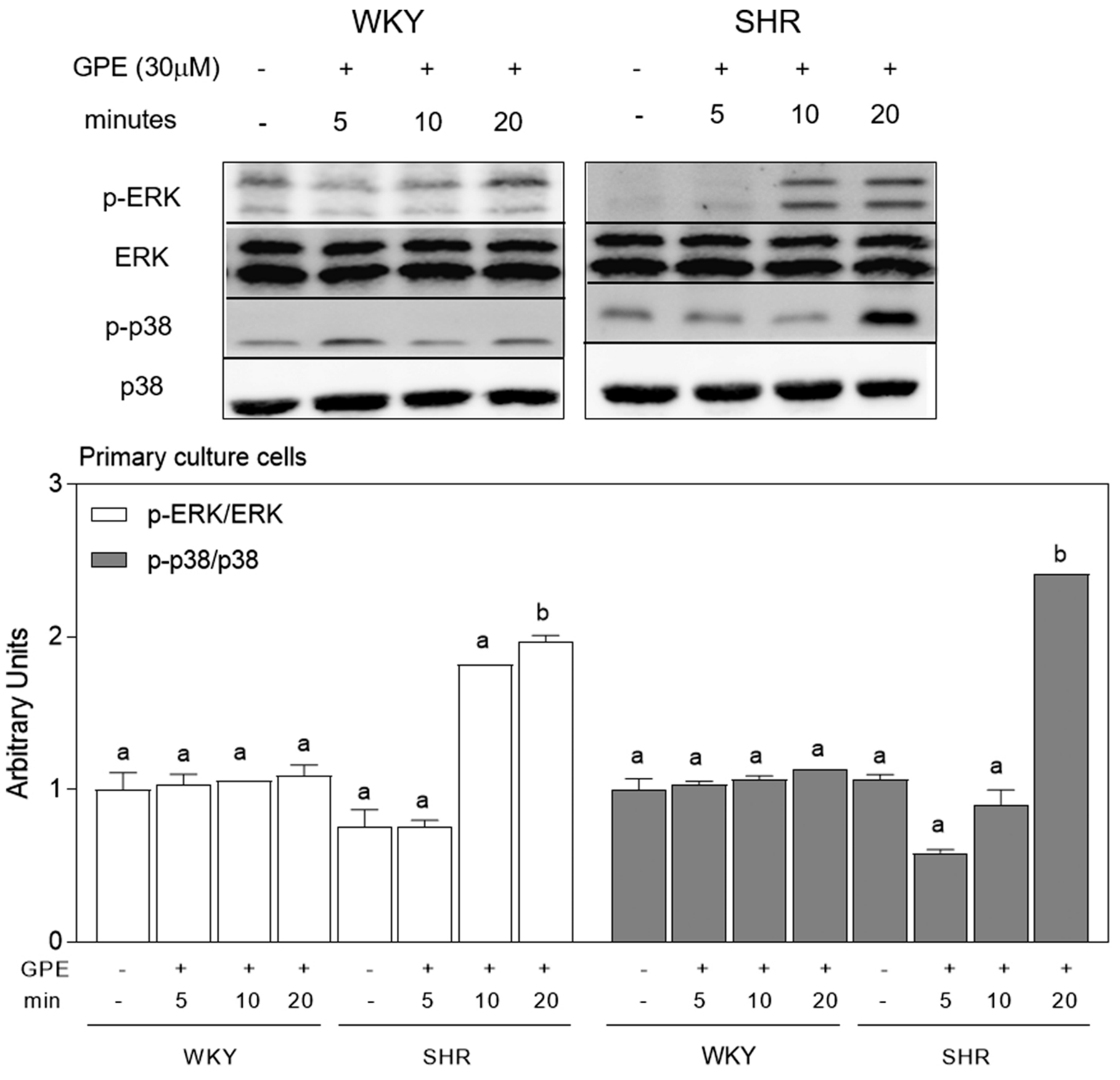
WKY
SHR
GPE (30μM) - + + + - + + +
minutes - 5 10 20 - 5 10 20
p-ERK
ERK
p-p38
p38
Primary culture cells
p-ERK/ERK
p-p38/p38
Arbitrary Units
0
1
2
3
a a a a a a a b
a a a a a a a b
GPE - + + + - + + + - + + + - + + +
min - 5 10 20 - 5 10 20 - 5 10 20 - 5 10 20
WKY SHR WKY SHR

Figure 6